JOURNAL OF SOLID STATE CHEMISTRY **122,** 315–320 (1996)
ARTICLE NO. 0119

# X-Ray and $^{23}$Na NMR Investigations on $Na^+$– and $Na^+/La^{3+}$–$\beta''$-$Al_2O_3$ Crystals

J. Köhler, G. Balzer-Jöllenbeck, and W. Urland

*Universität Hannover, Institut für Anorganische Chemie and SFB 173, Callinstraße 9, 30167 Hannover, Germany*

Received July 21, 1995; in revised form November 9, 1995; accepted December 19, 1995

**The structure of a $Na^+/La^{3+}$–$\beta''$-$Al_2O_3$ crystal (degree of exchange $\xi = 80\%$) has been investigated by conventional single crystal X-ray diffraction methods at room temperature. The lanthanide ions occupy eightfold ccordinated mO (9*d*) as well as sevenfold coordinated BR sites (6*c*). Remaining $Na^+$ ions were found exclusively in BR positions. $^{23}$Na NMR measurements were performed at room temperature before and after the exchange procedure. Two distinct $^{23}$Na signals differing in angular dependence of the second order quadrupole resonance shifts were recorded for the pure $Na^+$–$\beta''$-$Al_2O_3$ crystal whereas in the case of the doped isomorph only one signal was detected. The $^{23}$Na NMR signals were assigned to the two possible positions for the $Na^+$ ions in the conduction planes.** 

## INTRODUCTION

The structure of the superionic conductor $Na^+$–$\beta''$-alumina consists of layers of close-packed oxygen ions with $Mg^{2+}$ and $Al^{3+}$ ions in tetrahedral and octahedral sites (the so-called spinel blocks) separated by loosely packed layers containing the $Na^+$ ions (the so-called conduction planes). The spinel blocks are connected by covalent Al–O–Al bonds as well as by cationic Coulomb attraction forces (1). Due to the high mobility within these planes the $Na^+$ ions are exchangeable by other mono-, di-, and trivalent cations, in particular by trivalent lanthanide ions (2). Possible positions taken by the cations in the planes are the sevenfold coordinated Beevers–Ross (BR) site ($C_{3v}$ symmetry, 6*c* Wyckoff notation in $R\bar{3}m$) and the eightfold coordinated mid-Oxygen (mO) site ($C_{2h}$ symmetry, 9*d*) (Fig. 1). $Na^+$ ions in undoped $Na^+$–$\beta''$-$Al_2O_3$ crystals occupy both positions but the detailed distribution, especially the mO/BR occupancy ratio determined by X-ray diffraction methods, differs in the literature due to distinct crystal compositions and heat treatments during and after the synthesis procedure (1, 3–4). On the other hand, in completely lanthanide ion exchanged $\beta''$-alumina crystals the cationic arrangement is reported concurrently with the lanthanide ions occupying mostly the higher coordinated mO sites (5–7).

Several $^{23}$Na NMR studies have been performed on $Na^+$–$\beta''$-alumina in order to get a detailed picture of the dynamics taken place within the conduction planes (i.e., information about number of occupied sites, local cationic disordering, charge distributions, site symmetries, etc.) (8–10). The purpose of this paper is to determine in an *in situ* experiment the nuclear magnetic response of $Na^+$ ions occupying either mO or BR sites. Hence, a $La^{3+}$ ion-doped $Na^+$–$\beta''$-$Al_2O_3$ crystal has been investigated by taking $^{23}$Na NMR spectra before and after the exchange procedure. Single crystal X-ray diffraction methods were used to determine the structure and to verify the cationic distribution in the conduction planes for a definite signal-to-site assignment.

## EXPERIMENTAL

Single crystals of $Na^+$–$\beta''$-$Al_2O_3$ were synthesized by flux evaporation in a $Na_2O$ rich flux at a temperature of 1690°C (11). Anhydrous $LaCl_3$ powder has been prepared by the ammonium chloride route (12). The investigated crystal was ion exchanged by immersion in a $LaCl_3$/NaCl melt (molar ratio 50 : 50) at 700°C for 3 h under an argon atmosphere. The crystal composition and the degree of exchange ($\xi$) were determined before and after the ion exchange by electron probe microanalysis (Cameca Camebax). X-ray intensity measurements were taken at room temperature on a four-circle diffractometer. Experimental data are listed in Table 1.

$^{23}$Na NMR spectra were recorded in a 4.698 T magnetic field on a Bruker NMR spectrometer (model MSL 200) at room temperature. To suppress the $^{63}$Cu NMR signal and for getting a better filling factor of the NMR coil the standard Bruker probe head was modified by installing a silver coil with an inner diameter of 4 mm. For improving the signal to noise ratio 12,000 to 37,000 scans were accumulated with a repetition time of 0.3 s and a pulse length of 1.5 $\mu$s. The orientation of the crystal relative to the applied magnetic field is given by two angles, $\Theta$ defining the angle between the *c* axis and the magnetic field vector **B** and $\varphi$ for the angle between the *a* axis and the rotation



0022-4596/96 $18.00

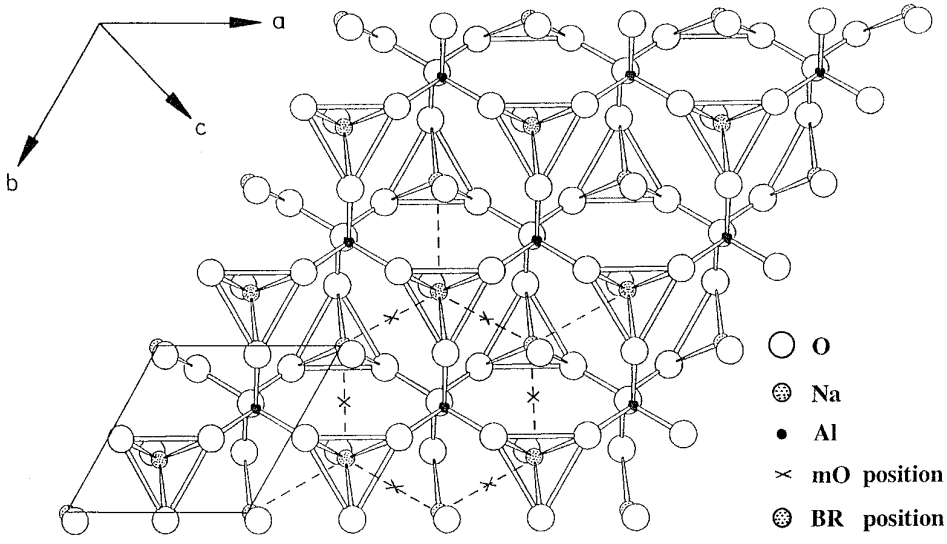


**FIG. 1.** *ab* conduction plane in $Na^+$–$\beta''$-alumina. The unit cell is given by the solid lines.

axis lying in the *ab* plane. Θ could be set anywhere in the range between 0° and 180° with an uncertainty of less than 2°. Rotation patterns (second order quadrupole resonance shift $\Delta\nu^{(2)}$ of the central transition $1/2 \leftrightarrow -1/2$ versus Θ) were recorded by rotating the crystal perpendicular to *c* with $\varphi = 0°$ (rotation axis parallel to *a*) and $\varphi = 90°$ (rotation axis perpendicular to *a*).

**TABLE 1**
**Data Collection and Refinement Parameters for $Na_{0.21}La_{0.44}Mg_{0.72}Al_{10.34}O_{17}$**

| | |
|---|---|
| Cell parameters (pm) | $a$ = 561.4(1), $c$ = 3352.5(5) |
| Space group | $R\bar{3}m$ |
| Formula units per unit cell | 3 |
| $\rho$(g · cm$^{-3}$) | 3.484 |
| Crystal dimension (mm) | 0.23 × 0.57 × 0.03 |
| Four-circle diffractometer | Siemens–Stoe AED2 |
| Radiation | Mo$K\alpha$ ($\lambda$ = 71.073 pm) |
| Intensity measurement method | $\omega$-2Θ scan |
| Degree intervals per step | 35 steps of 0.03° |
| 2Θ range | 3.64° ≤ 2Θ ≤ 58.02° |
| Min./max. *hkl* | ±(7 7 45) |
| No. of observed reflections | 3185 |
| No. of unique reflections | 360 |
| No. of rejected reflections | 0 |
| Linear absorption factor | 25.9 |
| Absorption correction | empirical |
| Program used | STRUCSY (16),[a] SHELXL-93 (17) |
| Refinement | full-matrix least-squares, based on $F^2$ |
| Refined parameter | 58[b] |
| $R1$, w$R2$[c] | 0.0358, 0.0799 (no $\sigma$ limit) |
| GooF = $S$ | 1.111 |
| max. $\|\Delta\|/\sigma$ | 0.000 |
| min./max $\Delta\rho$[e · pm$^{-3}$ · 10$^{-6}$] | −0.34/1.05 |

[a] Data reduction and correction of intensities.
[b] Including extinction coefficient.
[c] Definition of $R1$, w$R2$, $S$ in (17).

## REFINEMENTS

Starting parameters used in the least-squares structure refinements of the spinel blocks and column oxygens were taken from Ref. (1). The two remaining peaks at mO and BR positions in the difference Fourier synthesis were interpreted to result from $La^{3+}$ in mO and $Na^+$ in BR sites. To correspond to the microprobe analysis $La^{3+}$ occupancy was also introduced at the BR site and refined together with $Na^+$. Atomic positions, site occupation factors, and displacement parameters of all cations within the conduction planes could be calculated independently and without any

**TABLE 2**
**Site Multiplicities, Occupation Factors, and Fractional Atomic Coordinates for $Na_{0.21}La_{0.44}Mg_{0.72}Al_{10.34}O_{17}$**

| Atom | Site | s.o.f. | *x/a* | *y/b* | *z/c* |
|---|---|---|---|---|---|
| La(1) | 6*c* | 0.085(4) | 0 | 0 | 0.1746(1) |
| Na(1) | 6*c* | 0.136(23) | 0 | 0 | 0.1706(16) |
| La(2) | 9*d* | 0.076(2) | 0.8333 | 0.1667 | 0.1667 |
| Al(1) | 3*a* | 1.0 | 0 | 0 | 0 |
| Al(2) | 6*c* | 0.984(7) | 0 | 0 | 0.3501(1) |
| Al(3) | 18*h* | 0.988(6) | 0.3347(1) | *x*/2 | 0.0717(1) |
| Al(4) | 6*c* | 1.0 | 0 | 0 | 0.4505(1) |
| O(1) | 18*h* | 0.987(8) | 0.1548(2) | 2*x* | 0.0343(1) |
| O(2) | 6*c* | 1.0 | 0 | 0 | 0.2951(1) |
| O(3) | 6*c* | 1.0 | 0 | 0 | 0.0971(1) |
| O(4) | 18*h* | 0.982(11) | 0.1637(1) | 2*x* | 0.2349(1) |
| O(5) | 18*g* | 0.931(21) | 0.4179(41) | 0.6667 | 0.1667 |

**TABLE 3**
**Anisotropic (for Ions in the Conduction Planes) and Equivalent (for Spinel Block Ions) Components of the Displacement Parameters ($pm^2$) for $Na_{0.21}La_{0.44}Mg_{0.72}Al_{10.34}O_{17}$**

| Atom | $U_{11}$ | $U_{22}$ | $U_{33}$ | $U_{12}$ | $U_{23}$ | $U_{13}$ | $U_{eq}$[a] |
|---|---|---|---|---|---|---|---|
| La(1) | 113(18) | 113(18) | 103(15) | 0,5 × $U_{11}$ | 0 | 0 | |
| Na(1) | 2886(1045) | 2886(1045) | 621(276) | 0,5 × $U_{11}$ | 0 | 0 | |
| La(2) | 148(13) | 148(13) | 122(12) | −80(9) | −13(4) | 13(4) | |
| O(5) | 284(68) | 329(216) | 88(27) | 164(108) | −21(30) | −10(15) | |
| Al(1) | | | | | | | 90(4) |
| Al(2) | | | | | | | 99(4) |
| Al(3) | | | | | | | 98(3) |
| Al(4) | | | | | | | 100(4) |
| O(1) | | | | | | | 112(5) |
| O(2) | | | | | | | 113(5) |
| O(3) | | | | | | | 113(6) |
| O(4) | | | | | | | 107(6) |

[a] $U_{eq} = 1/3\ [U_{33} + 4/3\ (U_{11} + U_{22} - U_{12})]$ (18).

constraint. Alternative refinements with $Na^+$ in mO sites led to unreasonable site occupation factors and vanishing displacement parameters for the in-plane cations. This ionic distribution ($Na^+$ in mO) was not taken into account for further considerations. Finally, the bridging oxygens O(5) were displaced into 18*g* positions. $Al^{3+}$ and $O^{2-}$ ions in the spinel blocks were refined independently. Fully occupied positions were fixed subsequently in the final refinement. A distinction between $Al^{3+}$ and $Mg^{2+}$ was not possible due to the nearly equal atomic form factors. For keeping charge neutrality the $Mg^{2+}$ content could be estimated by the refined cationic/anionic occupancy ratio. Computations in the noncentrosymmetric space group *R*3*m* led to no significantly improved *R* values.

The fractional atomic parameters, the displacement parameters, and some interatomic distances are given in Tables 2, 3 and 4, respectively. Figure 2 displays the Fourier electron density map $\rho_{obs}$ of the conduction plane (*ab* plane) with $z = 0.17$)[1]

## RESULTS AND DISCUSSION

### *1. Crystal Structure*

The lattice parameter *c* of the 80% exchanged $Na^+/La^{3+}$–$\beta''$-$Al_2O_3$ crystal ($c = 3352.5(5)$ pm) is reduced in comparison to undoped $Na^+$–$\beta''$-alumina ($c = 3385$ pm (1)) due to the higher Coulomb attraction forces of the trivalent lanthanide ions to the spinel block anions. The *a* parameter ($a = 561.4(1)$ pm) is controlled by the rigid dimensions of the spinel block and remains uneffected by the ion exchange (561.4 pm for $Na^+$–$\beta''$-$Al_2O_3$ (1)). The electron microprobe analysis of the crystal led to $Na_{1.58\pm0.03}Mg_{0.68\pm0.06}Al_{10.35\pm0.05}O_{17}$ before and $Na_{0.21\pm0.02}La_{0.44\pm0.02}Mg_{0.72\pm0.03}Al_{10.34\pm0.01}O_{17}$ after the ion exchange procedure. Remarkably, nearly 80% of the $Na^+$ ions were replaced by $La^{3+}$ ions despite an equivalent molar $La^{3+}/Na^+$ ratio of the employed chloride melt. The accumulation of $La^{3+}$ ions is due to their restricted mobility within the conduction planes of the crystal.

In the refined crystal composition of $Na_{0.27\pm0.05}La_{0.40\pm0.01}Al_{10.91\pm0.05}O_{16.74\pm0.13}$ a negative deficit of 0.72 ± 0.15 electrons per formula unit is found. From neutron diffraction measurements on $Mg^{2+}$-stabilized $Na^+$–$\beta''$-$Al_2O_3$ crystals it is known that $Mg^{2+}$ substitutes $Al^{3+}$ at the tetrahedral Al(2) site close to the centers of the spinel blocks (13). Hence, attributing the charge disproportion to $Mg^{2+}$ ions the composition results after substraction from the $Al^{3+}$ content in $Na_{0.27\pm0.05}La_{0.04\pm0.01}Mg_{0.72\pm0.15}Al_{10.19\pm0.05}O_{16.74\pm0.13}$ in reasonable agreement with the microprobe analysis. As can be seen from Fig. 2 the electron density is extended for all positions in the conduction planes indicating large local disordering. The

**TABLE 4**
**Selected Interatomic Distances (pm) in $Na_{0.21}La_{0.44}Mg_{0.72}Al_{10.34}O_{17}$**

| | | | | | |
|---|---|---|---|---|---|
| La(1)–O(5) | 285.2(19) | 3× | Al(1)–O(1) | 189.3(1) | 6× |
| La(1)–O(4) | 257.3(3) | 3× | Al(2)–O(1) | 183.2(1) | 3× |
| La(1)–O(3) | 259.8(4) | 1× | Al(2)–O(2) | 184.6(3) | 1× |
| Na(1)–O(5) | 284.3(19) | 3× | Al(3)–O(4) | 183.7(1) | 2× |
| Na(1)–O(4) | 268.1(42) | 3× | Al(3)–O(3) | 183.6(1) | 1× |
| Na(1)–O(3) | 246.3(53) | 1× | Al(3)–O(2) | 196.5(2) | 1× |
| La(2)–O(5) | 233.2(23) | 2× | Al(3)–O(1) | 200.9(1) | 2× |
| La(2)–O(4) | 279.5(1) | 4× | Al(4)–O(5) | 172.6(6) | 1× |
| La(2)–O(3) | 284.0(2) | 2× | Al(4)–O(4) | 176.4(1) | 3× |

[1] Further details of the crystal structure investigation can be requested at the FACH-INFORMATIONSZENTRUM KARLSRUHE, 76344 Eggerstein-Leopoldshafen 2, by giving the deposit number CSD-404217.

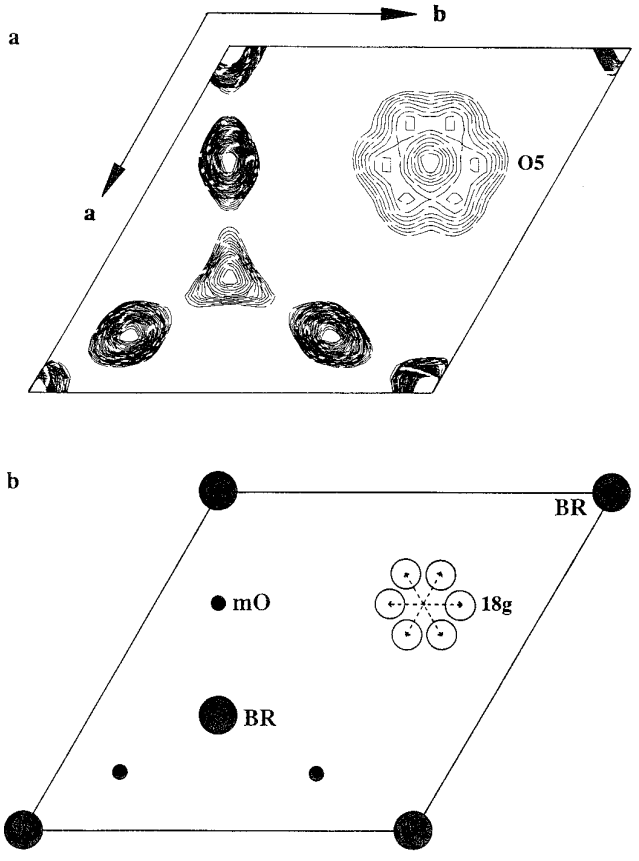


**FIG. 2.** (a) Fourier electron density map $\rho_{obs}$ of the conduction plane in $Na_{0.21}La_{0.44}Mg_{0.72}Al_{10.34}O_{17}$. The contour intervals are 2.0 e/pm$^6$. (b) A schematic representation of the occupied sites in $Na_{0.21}La_{0.44}Mg_{0.72}Al_{10.34}O_{17}$.

bridging oxygens O(5) are displaced 47.5 pm from the 3*b* toward occupied mO positions into 18*g* sites resulting in bent Al–O–Al bridges and a decreased lattice parameter *c*. Cations in 9*d* (mO) show a large anisotropic displacement parameter in the direction of neighbored empty BR sites whereas cations in 6*c* (BR) are attracted toward the spinel block anions (*c* direction). $La^{3+}$ ions occupy mO as well as, together with $Na^+$, BR sites. The $Na^+$ ions are less attracted to the spinel block ions due to their lower charge: $z_{Na^+} = 0.1706$, $z_{La^{3+}} = 0.1746$. Furthermore, the $Na^+$ ions are slightly shifted from the 6*c* position (BR) in the direction of an 18*h* site as indicated by the large in-plane components of the anisotropic displacement parameter ($U_{11}$, $U_{22}$). The unusual high values of $U_{ij}(Na^+)$ may be caused by the difficulty for the used structure refinement program to differentiate the electron density between the large $La^{3+}$ and the small $Na^+$ contributions within the same site. Attempts to constrain the $Na^+$ displacement parameters result in increased *R* values and crystal compositions differing significantly from the microprobe analysis.

A high $La^{3+}$ fraction of 43% is found in the smaller Beevers–Ross sites. This is remarkable as normally the lanthanide ions, especially the lighter ones, predominantly prefer the higher coordinated mO sites (5). Also, in lower exchanged crystals a significant BR occupancy (26%) is found (6). The discrepancy between published data and the BR occupancy found in this work is interpreted to result from differently composed undoped $Na^+$–$\beta''$-$Al_2O_3$ crystals used for the ion exchange. A varying $Na^+$ content influences the value of the lattice parameter *c* connected with the shrinkage or expansion of the conduction slabs. Low $Na^+$ concentrations lead to widened conduction slabs resulting in higher BR occupancies by the incorporated lanthanide ions as can be found in completely exchanged $Na^+/Pr^{3+}$–$\beta''$-$Al_2O_3$ (14).

### 2. $^{23}$*Na NMR Measurements*

The $Na^+$ resonance line is perturbed by the interaction of the electric quadrupole moment of the $Na^+$ nuclei with the electric field gradient (efg) at the corresponding crystallographic position. Due to strong first order quadrupole interactions in $Na^+$–$\beta''$-$Al_2O_3$ only the central spin transition $1/2 \leftrightarrow -1/2$ could be observed. At room temperature small shifts of the $Na^+$ ions from the mean positions as indicated by high thermal vibrations are averaged and the corresponding resonance lines merge to a single line position. In this case the frequency shift $\Delta\nu_{1/2}^{(2)}$ of the central transition for a spin 3/2 nucleus perturbed in second order is given by

$$\Delta\nu_{1/2}^{(2)} = -(3\nu_Q^2/192\nu_L)(4A\cos^4\Theta + B\cos^2\Theta + C) \quad [1]$$

with $A = -81 - 4.5\,\eta^2$, $B = 90 - 3\,\eta^2$, $C = -9 + 3.5\,\eta^2$, and the quadrupole coupling constant $\nu_Q = e^2qQ/2h$. $\nu_L$

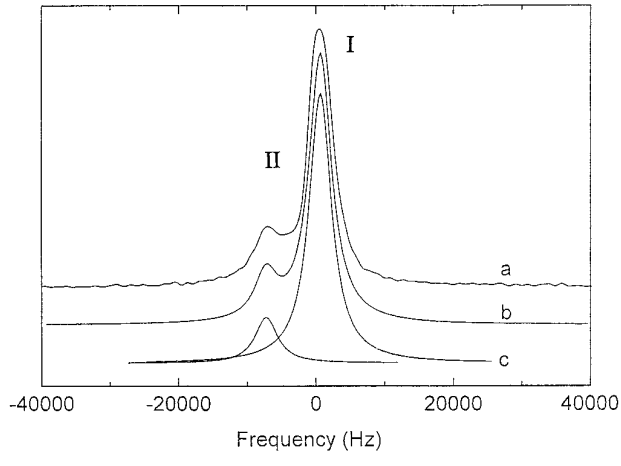


**FIG. 3.** (a) $^{23}$Na NMR spectrum of the central transition $1/2 \leftrightarrow -1/2$ of $Na_{1.58}Mg_{0.68}Al_{10.35}O_{17}$ at room temperature for $\Theta = 141°$ and $\varphi = 0°$ ($\Delta\nu_{1/2}^{(2)} = 0$ is chosen for $\Theta = 0°$). (b) Simulation assuming two overlapping Lorentzian lines. (c) The deconvoluted spectrum.

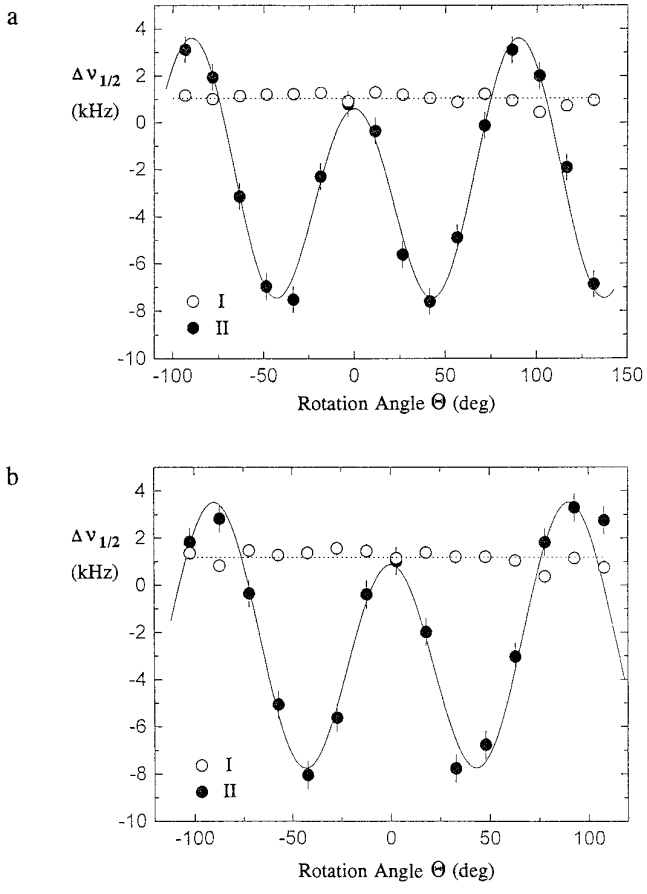


**FIG. 4.** (a) Room temperature rotation pattern of the second order quadrupole shift ($\Delta\nu_{1/2}$) for the transition $1/2 \leftrightarrow -1/2$ of $^{23}Na$ in $Na_{1.58}Mg_{0.68}Al_{10.35}O_{17}$ as a function of Θ with the rotation axis parallel to $a$ ($\varphi = 0°$) and (b) with the rotation axis perpendicular to $a$ ($\varphi = 90°$). The circles represent the experimental data (signal I and II, cf. Fig. 3) whereas the solid curve corresponds to the calculated shift from Eq. [1].

is the Larmor frequency of 52.939 MHz, Θ the angle of the magnetic field with respect to the crystallographic $c$ axis, $eq$ the electric field gradient, $\eta$ the asymmetry parameter, and $Q$ the nuclear quadrupole moment (15).

In Fig. 3 the $^{23}Na$ NMR spectrum of the undoped $Na^+$–$\beta''$-$Al_2O_3$ crystal is shown. Two signals are recognizable resulting from $Na^+$ ions occupying the two different crystallographic BR and mO positions. The main features of the spectrum are simulated by two superimposed Lorentzian shaped lines. In Fig. 4a the frequency shifts $\Delta\nu_{1/2}^{(2)}$ of both fitted signals are plotted versus the rotation angle Θ. For signal I the frequency shift is nearly constant within the measured angle region indicating a small or vanishing electric field gradient, whereas $\Delta\nu_{1/2}^{(2)}$ of signal II shows a significant Θ dependence resulting from a larger efg at this position. By using a nonlinear least-squares algorithm the frequency shifts $\Delta\nu_{1/2}^{(2)}$ were fitted by Eq. [1] (cf. the solid lines in Fig. 4) resulting in a quadrupole coupling constant $\nu_Q = 2.20 \pm 0.05$ MHz and an asymmetry parameter $\eta = 0.68 \pm 0.10$. Within the standard deviations the same results are obtained after rotating the crystal 90° around the $c$ axis ($\varphi = 90°$), as can be seen from the similar rotation pattern in Fig. 4b ($\nu_Q = 2.16 \pm 0.05$ MHz and $\eta = 0.57 \pm 0.12$).

Comparing the symmetry of the two possible crystallographic sites within the conduction planes a stronger electric field gradient is to be expected for the lower symmetric mO position. The first coordination sphere of the BR site in unexchanged $Na^+$–$\beta''$-$Al_2O_3$ presents a slightly distorted tetrahedron of four spinel block oxygen ions (averaged $Na_{BR}$–$O_{spinel}$ distance: 284 pm (1)). The three more distant column oxygens O(5) ($Na_{BR}$–O(5) distance: 325 pm (1)) complete the aforementioned sevenfold coordination. Cations within the distorted tetrahedral coordination sphere experience due to the nearly cubic symmetry only a vanishing electric field gradient. On the other hand, for the mO site the bridging oxygens O(5) represent the nearest neighbors of the noncubic eightfold coordination (averaged $Na_{mO}$–$O_{spinel}$ distance: 284 pm, $Na_{mO}$–O(5) distance: 281 pm (1)) generating a strong efg. So, signal I is related to $Na^+$ ions occupying BR positions whereas the Θ-dependent signal II refers to $Na^+$ ions residing in mO sites. To verify these assumptions a fraction of $Na^+$ was replaced by $La^{3+}$ ions and the so obtained crystal was investigated by $^{23}Na$ NMR measurements, again. $La^{3+}$ was chosen for the $Na^+$ exchange because of its absent paramagnetic property and the known behavior of the preferential mO occupancy by larger lanthanide ions (5–7). Replacing all $Na^+$ ions within this site only one $^{23}Na$ NMR signal should be observed. Figure 5 displays the resulting spectrum after the ion exchange compared with the data of the undoped $Na^+$–$\beta''$-$Al_2O_3$ crystal. Indeed, after $La^{3+}$ exchange one $^{23}Na$ NMR

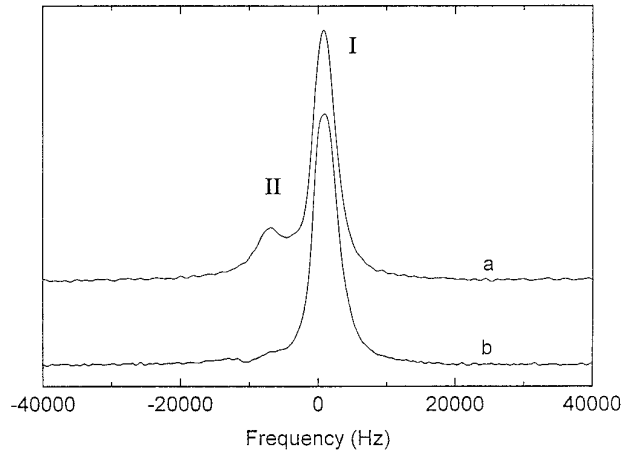


**FIG. 5.** (a) $^{23}Na$ NMR spectra for $Na_{1.58}Mg_{0.68}Al_{10.35}O_{17}$ and (b) $Na_{0.21}La_{0.44}Mg_{0.72}Al_{10.34}O_{17}$ at $\Theta = 42°$, where the maximal splitting of the two lines is found ($\varphi = 0°$).

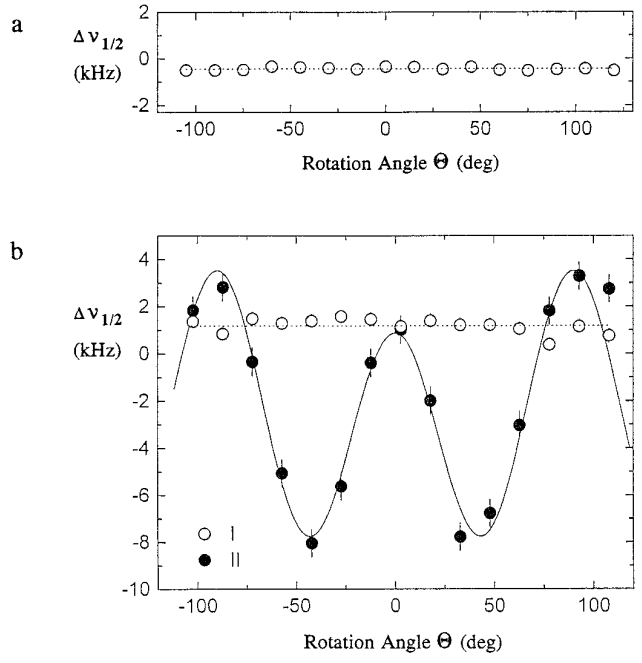


**FIG. 6.** Comparison of the room temperature rotation pattern of the second order quadrupole shift ($\Delta\nu_{1/2}$) for the central transition $1/2 \leftrightarrow -1/2$ of $^{23}Na$ (a) in $Na_{0.21}La_{0.44}Mg_{0.72}Al_{10.34}O_{17}$ and (b) in $Na_{1.58}Mg_{0.68}Al_{10.35}O_{17}$ as a function of $\Theta$ ($\varphi = 0°$).

signal (the Θ-dependent one) has disappeared indicating a complete removal of $Na^+$ ions from the corresponding site. The remaining signal shows the same resonance position and frequency shift dependence on the rotation angle Θ as signal I in the undoped crystal as can be seen from Fig. 6. Hence, it is attributed to $Na^+$ ions within the higher symmetrical BR site experiencing no or a vanishing electric field gradient. These assumptions are confirmed by the X-ray results mentioned above in which a $Na^+$ occupancy is found only for the BR positions. Although the $Na_{BR}$–O(5) distance in $Na_{0.21}La_{0.44}Mg_{0.72}Al_{10.34}O_{17}$ is reduced due to the O(5) displacements (see Table 4) the tetrahedral coordination for the BR site is still conserved. Slight shifts of $Na^+$ ions toward 18*h* sites as indicated by the large components of the anisotropic displacement parameters are averaged at room temperature in the NMR and X-ray experiments giving the mean 6*c* (BR) position.

## CONCLUSIONS

In undoped $Na^+$–$\beta''$-$Al_2O_3$ the $Na^+$ ions occupy two crystallographic positions (BR and mO) giving rise to two signals in $^{23}Na$ NMR spectroscopy at room temperature. These signals differ in their dependency upon the crystal orientation relative to the applied magnetic field (Θ dependence). After a partial ion exchange with $La^{3+}$ ions, replacing $Na^+$ in mO, the residual $Na^+$ ions occupy only BR sites generating a single Θ-independent $^{23}Na$ NMR signal.

## ACKNOWLEDGMENT

We thank the Deutsche Forschungsgemeinschaft for financial support.

## REFERENCES

1. M. Bettman and C. R. Peters, *J. Phys. Chem.* **73,** 1774 (1969).
2. B. Dunn and G. C. Farrington, *Solid State Ionics,* **9–10,** 223 (1983).
3. J. P. Boilot, G. Collin, Ph. Colomban, and P. Comes, *Phys. Rev. B* **22,** 5912 (1980).
4. K. G. Frase, J. O. Thomas, and G. C. Farrington, *Solid State Ionics* **9–10,** 307 (1983).
5. W. Carrillo-Cabrera, J. O. Thomas, and G. C. Farrington, *Solid State Ionics* **28–30,** 317 (1988).
6. M. Wolf and J. O. Thomas, *J. Mater. Chem.* **4,** 839 (1994).
7. W. Carrillo-Cabrera, J. O. Thomas, and G. C. Farrington, *Solid State Ionics* **18–19,** 645 (1986).
8. K. R. Carduner, G. C. Farrington, D. White, and M. Villa, *Solid State Ionics* **9–10,** 339 (1983).
9. K. R. Carduner and D. White, *J. Chem. Phys.* **85,** 3165 (1986).
10. C. E. Hayes and D. C. Ailion, *Solid State Ionics* **5,** 233 (1981).
11. F. Tietz, J. Koepke, and W. Urland, *J. Cryst. Growth* **118,** 314 (1992).
12. G. Meyer, *Inorg. Synth.* **25,** 146 (1989).
13. G. M. Brown, D. A. Schwinn, J. B. Bates, and W. E. Brundage, *Solid State Ionics* **5,** 147 (1981).
14. J. Köhler and W. Urland, Ph.D. Thesis, Universität Hannover, 1996.
15. I. Chung and H. S. Story, *J. Chem. Phys.* **63,** 4903 (1975).
16. Siemens–Stoe, "STRUCSY, Programmsystem zur Lösung von Kristallstrukturen." Darmstadt.
17. G. M. Sheldrick, "SHELXL-93, A program for crystal structure refinement." Universität Göttingen, 1993.
18. R. X. Fischer and E. Tillmanns, *Acta Crystallogr. Sect. C* **44,** 775 (1988).